CrystEngComm

Accepted Manuscript

ROYAL SOCIETY OF CHEMISTRY

www.rsc.org/crystengcomm

Four Binuclear Coordination Polymers with 6^3 Net and Self-Assembly of 2D 6^3 Topology into Different Supramolecular Networks Using Unit-Unit H-Bonds

Guohai Xu,* Min Xie, Xiaokang Li,* Wenjie Shi, Hui Yu, Yinhui Hu, Xiaochen Xun, and Yongrong Xie*

Key Laboratory of Jiangxi University for Functional Materials Chemistry, School of Chemistry and Chemical Engineering, Gannan Normal University, Ganzhou, Jiangxi 341000, People's Republic of China

E-mail: xugh308@gnnu.cn; gnnulxk@163.com; xieyr@gnnu.edu.cn

Abstract

In this work, crystal engineering is focused on the self-assembly of 2D 6^3 topology into different supramolecular networks using unit-unit H-bonds. Four related coordination polymers, $[Zn_2(teaH_2)(ndc)_{1.5}]\cdot MeOH$ (**1**), $[Co_2(teaH_2)(ndc)_{1.5}]\cdot MeOH$ (**2**), $[Zn_2(deaH)(ndc)_{1.5}]\cdot MeOH$ (**3**) and $[Co_2(teaH_2)(btb)]\cdot 3EtOH$ (**4**) where ndc^{2-} = 2,6-naphthalenedicarboxylate, btb^{3-} = benzene-1,3,5-tribenzoate, $teaH_3$ = triethanolamine, and $deaH_2$ = diethanolamine, contain a well-known 6^3 subnet and the binuclear units. Furthermore, their 6^3 nets present different hexagonal window (chair- or ship-shaped) and diversified layer array (ABAB or ABCABC sequence). The 6^3 subnet and symmetry-related unit-unit H-bonds as supramolecular synthons can build up different supramolecular networks. Compounds **1**-**2** show a distorted diamond supramolecular network due to form a square-pyramidal node. Because of the formation of a seesaw-shaped node, compound **3** features a general diamond supramolecular network with 3-fold interpenetration. Compound **4** exhibits a binodal

supramolecular framework in that H-bonding interactions are happened among three binuclear units. In addition, the diversified layer array has endowed compound **4** with a large 1D channel, which can be characterized by standard N_2 adsorptions. Compound **4** has a type **I** adsorption isotherm with an appreciable adsorption of 45.04 cm^3g^{-1} at 0.40 P/P_0, whereas **1-3** do not exhibit appreciable N_2 uptake.

Introduction

Crystal engineering aims to construct crystalline solids with a predefined molecular organization and to convey desirable properties.[1] The rapid development of coordination polymers (CPs) has illumined the perspective to rationally realize the predicted structures.[2] A common concept is that one should design the suitable molecular building blocks and understand the interactions between them.[3] Therefore, both intermolecular interactions and molecular fragments are defined as "supramolecular synthons" by Desiraju.[4] Hydrogen bond (H-bond) is seemed as the most important form of intermolecular interactions.[5] In this aspect, special enthusiasm has been exceedingly paid to organic crystal engineering.[6] The system involving CPs has recently seen a burgeoning research in crystal engineering.[7] An objective of the present work is to probe the relations between H-bonding interactions and supramolecular topologies for CPs.

As we know, the CPs family has attracted considerable attentions for their intriguing structures. One of the most appealing aspects is attributed to their topological aesthetics.[8] Topological research on CPs has showed that three most common topologies of 2D coordination networks are regular 4^4, 6^3, and 3^6 nets.[2a, 9]

The 6^3 net, also termed **hcb** topology,[10] has a planar honeycomb-like shape with three-connected nodes. A challenging issue for producing desirable 6^3 net is to achieve the defined three-connected node. The cooperation of polyalcohol amines and organic carboxylates can contribute to the formation of a stable binuclear unit as three-connected node.[2d] Moreover, it has been testified that polyalcohol amines can serve as an excellent candidate for hydrogen-bond donation.[2d, 11] This strategy will endow the resultant complexes with predefined molecular blocks and intermolecular H-bonds.[11h] In this work, four binuclear coordination polymers with 6^3 net have been isolated in this protocol and characterized by the X-ray diffraction method, namely, $[Zn_2(teaH_2)(ndc)_{1.5}]\cdot MeOH$ (**1**), $[Co_2(teaH_2)(ndc)_{1.5}]\cdot MeOH$ (**2**), $[Zn_2(deaH)(ndc)_{1.5}]\cdot MeOH$ (**3**) and $[Co_2(teaH_2)(btb)]\cdot 3EtOH$ (**4**) where ndc^{2-} = 2,6-naphthalenedicarboxylate, btb^{3-} = benzene-1,3,5-tribenzoate, $teaH_3$ = triethanolamine, and $deaH_2$ = diethanolamine. Herein, 6^3 net and H-bonds act as supramolecular synthons. Crystal engineering is focused on the self-assembly of 2D 6^3 topology into different supramolecular networks using unit-unit H-bonds. We report their syntheses, structures, and N_2 adsorptions.

Experimental Section

Materials and physical measurements: The reagents needed for the syntheses are triethanolamine [$C_6H_{15}NO_3$ Aladdin (Shanghai), 98%], diethanolamine [$C_4H_{11}NO_2$ Aladdin (Shanghai), 98%], 2,6-naphthalenedicarboxylic acid [$C_{12}H_8O_4$ Aladdin (Shanghai), 99%], benzene-1,3,5-tribenzoate acid [$C_{27}H_{18}O_6$ Aladdin (Shanghai), 99%], $Zn(NO_3)_2\cdot 9H_2O$ [Aladdin (Shanghai), 98%], and $Co(NO_3)_2\cdot 6H_2O$ [Aladdin

(Shanghai), 98%]. The methanol and ethanol solvent were purchased from Sinopharm Chemical Reagent Co., Ltd. All reagents were used without further purification. CHN elemental analyses were conducted on a Perkin-Elmer 240C element analyzer. Powder X-ray diffraction data were collected using a Bruker D8 Advance (Cu Kα1 radiation, λ=1.5406 Å). Thermogravimetric analyses were performed using a Pyris Diamond thermal analyser. The Fourier transform IR spectra were recorded from KBr pellets in the range 4000-400 cm^{-1} on a Mattson Alpha-Centauri spectrometer. The N_2 adsorption isotherm was obtained on a BET surface area analyzer (ASAP-2020).

Synthesis of $[Zn_2(teaH_2)(ndc)_{1.5}]\cdot MeOH$ (1). A mixture of $Zn(NO_3)_2\cdot 9H_2O$ (0.0387 g, 0.13 mmol), $ndcH_2$ (0.0260 g, 0.13 mmol) and $teaH_3$ (0.18 mL) was dissolved in methanol (10 mL) under stirring. The resultant solution was transferred into a 17ml Teflon-lined stainless steel container and heated at 120°C for 36h. After cooling to room temperature, colorless block crystals of **1** were collected in 45.9% yield based on the added amounts of $Zn(NO_3)_2\cdot 9H_2O$. Anal. Calcd for $C_{25}H_{27}NO_{10}Zn_2$: C, 47.49; H, 4.30; N, 2.22, Found: C, 47.46; H, 4.32; N, 2.25. Selected IR data (KBr pellet, cm^{-1}): 486(w), 565(w), 640(w), 787(m), 897(w), 1060(m), 1190(w), 1410(s), 1610(s), 2860(w).

Synthesis of $[Co_2(teaH_2)(ndc)_{1.5}]\cdot MeOH$ (2). **2** was synthesized by a procedure similar to that used for **1** except that equal moles of $Co(NO_3)_2\cdot 6H_2O$ were used in place of $Zn(NO_3)_2\cdot 9H_2O$. Yield: 66.1% based on the added amounts of $Co(NO_3)_2\cdot 6H_2O$. Anal. Calcd for $C_{25}H_{27}NO_{10}Co_2$: C, 48.48; H, 4.39; N, 2.26, Found: C, 48.50; H, 4.41; N, 2.26. Selected IR data (KBr pellet, cm^{-1}): 478(w), 557(w),

706(w), 781(m), 856(w), 1060(m), 1390(s), 1540(m), 1590(s), 2850(w).

Synthesis of $[Zn_2(deaH)(ndc)_{1.5}]\cdot MeOH$ (3). **3** was synthesized by a procedure similar to that used for **1** except that equal volumes of $deaH_2$ were used in place of $teaH_3$. Yield: 58.4% based on the added amounts of $Zn(NO_3)_2\cdot 9H_2O$. Anal. Calcd for $C_{23}H_{23}NO_9Zn_2$: C, 46.96; H, 3.94; N, 2.38, Found: C, 46.97; H, 3.96; N, 2.35. Selected IR data (KBr pellet, cm^{-1}): 488(m), 596(w), 789(s), 924(m), 1050(m), 1190(m), 1410(s), 1570(s), 2870(w).

Synthesis of $[Co_2(teaH_2)(btb)]\cdot 3EtOH$ (4). **4** was synthesized by a procedure similar to that used for **2** except that equal moles of $btbH_3$ were used in place of $ndcH_2$, and equal volumes of EtOH in place of MeOH. Yield: 72.7% based on the added amounts of $Co(NO_3)_2\cdot 6H_2O$. Anal. Calcd for $C_{39}H_{47}NO_{12}Co_2$: C, 55.78; H, 5.64; N, 1.67, Found: C, 55.80; H, 5.65; N, 1.67. Selected IR data (KBr pellet, cm^{-1}): 455(m), 553(w), 638(m), 783(s), 893(w), 1060(m), 1190(w), 1350(s), 1410(s), 1610(s), 2850(w).

Single crystal structure determination: A Bruker Apex II CCD diffractometer equipped with graphite monochromatized Mo Kα radiation (λ = 0.71069 Å) was used to collect X-ray intensity data. Diffraction intensities for compounds **1-4** were collected on 298 K. Absorption corrections were applied using the multi-scan technique.[12] The structures were solved by direct methods using SHELXS-97[13] and refined with full-matrix least-squares techniques using the SHELXL-97 program[14] within WINGX.[15] All non-hydrogen atoms were refined anisotropically. All C-bound H atoms were refined using a riding model. The hydroxy H atoms of solvent

molecules were placed geometrically and refined as riding modes. The hydroxy H atoms of ethanol arms on $teaH_2^-$/$deaH^-$ anions were located in a difference Fourier map and their positions were refined under the application of an O-H bond-length restraint of 0.90(1), with Uiso(H) values set at 1.5Ueq(O). Experimental details of the X-ray analyses are provided in Table 1.

Results and Discussion

Crystal structures of compounds 1 and 2. Selected bond lengths and bond angles as well as the detailed hydrogen bonds for compounds **1**-**4** are given in Tables 2 and 3. X-ray diffraction structural analyses reveal that compound **1** isostructural to **2** and their 2D architectures are made from binuclear metal units (M = Zn^{II}, Co^{II}) and ndc^{2-} connectors. Hence, only the structure of **1** will be representatively discussed in detail. Compound **1** crystallizes in the centrosymmetric space group P-1. As shown in Figure 1a, there are one mono-deprotonated $teaH_2^-$ ligand, three of half an ndc^{2-} anions, and one free methanol molecule as well as two crystallographically independent Zn^{II} centers in the asymmetric unit. The ndc^{2-} ligand shows three types of coordination modes (tetradentate bridging: μ_4-$\kappa^1\kappa^1\kappa^1\kappa^1$, bis(monodentate): μ_2-$\kappa^1\kappa^1$ and tetradentate chelating: μ_2-$\kappa^1\kappa^1\kappa^1\kappa^1$ in Chart 1). All ndc^{2-} anions are on inversion centers that occur at the co-edged centroids of naphthyl rings. The Zn_2 unit is held together through the chelating-bridging (N, O, O', μ_2-O'') $teaH_2^-$ ligand and the bidentate bridging COO^- group. Each Zn_2 unit is connected to three adjacent ones via naphthyl fragments of ndc^{2-} ligands so that a three-connected node appears (Figure 1b). Finally, the three-connected uninodal entity results in a layered 6^3 net with cavities surrounded by

six naphthyl trunks and six Zn_2 units (Figure 1c). In the Zn_2 unit, two Zn centers show five-coordination geometry with different τ values (0.246 and 0.689 for Zn1 and Zn2).[16] The two τ values suggest that the Zn1 center is preferably described as distorted square-pyramidal geometry while another Zn2 atom adopts a distorted trigonal-bipyramidal environment. The O6 atom from one carboxyl group is located on the axial position of square-pyramid of Zn1 center. The two polar positions for Zn2 geometry are assigned to the O1 atom of one COO- group and the N1 atom of $teaH_2^-$ ligand. The Zn-N distance (2.164(3) Å for Zn2-N1) and the Zn-O bond lengths (ranging from 1.940(3) to 2.309(3) Å) are in the normal range for Zn complexes of $teaH_3$.[2d, 17]

It should be noticeable that each Zn_2 unit behaves as a tripod to connect with three Zn_2 units. Therefore, the resultant 6^3 net must present a puckered layer which contains a hexagonal $(—Zn_2\ unit—ndc—)_6$ window (Figure 1c). The hexagonal window shows a chair-shaped configuration in which the Zn_2 units are not all coplanar, rather, half fall in the above layer, half in the below layer (Figures 1c and S1a). The close packing tendency is satisfied by adopting an offset ABAB stacking arrangement where two MeOH guests reside in the remaining 12-membered cavities (Figure 1d). No interpenetration is found in compounds **1** and **2**.

The noteworthy feature for **1**-**2** is the H-bonding interactions which can self-assemble the 2D 6^3 net into a 3D supramolecular network. The polyhydroxyl arms of $teaH_2^-$ anions provide the binuclear units with great potential in hydrogen bonds. H-bonding analyses reveal that a pair of strong symmetry-related H-bonds ties

up two binuclear units from two adjacent 6^3 layers (Figure S1b and 2a). Taking the H-bonding interactions into account, the binuclear units can be regarded as four-connected uninodes. However, each four-connected uninode exhibits a square-pyramidal conformation so that the final nets of **1**-**2** are expanded into a distorted 3D diamond framework (Figure 2a and 2b).

Crystal structure of compound 3. The replacement of Zn by Co can not change the total structures of **1**-**2**. However, the use of diethanolamine results in structural variant and a new compound **3** is isolated. In compound **3**, the Zn_2 unit still remains stable and the 6^3 net also reappears (Figure 3). The asymmetric unit in **3** consists of two crystallographically independent Zn^{II} ions, one $teaH_2^-$ anion, and two types of ndc^{2-} anions (two of half an ndc^{2-} anions with μ_4-$\kappa^1\kappa^1\kappa^1\kappa^1$ mode, and half an ndc^- anion with μ_2-$\kappa^1\kappa^1$ mode) (Figure 3a). The $deaH_2^-$ anion adopts a (N, O, μ_2-O') conformation to chelate and bridge two Zn atoms. Compared with the Zn_2 unit of **1**, the two Zn centers exhibit different coordination geometry. One Zn2 atom completes the five-coordination environment by three coordinated atoms from $teaH_2^-$ anion and two O atoms from two ndc^{2-} anions. The τ value (0.195) indicates that the Zn2 center is a slightly distorted square-pyramidal geometry. The O3 atom from one carboxyl group resides on the axial position of square-pyramid. However, another Zn1 center is tetrahedrally coordinated by three O atoms from three ndc^{2-} anions and one μ_2-O atom of $teaH_2^-$ anion. The bond angles about the Zn1 center lie in the range of 98.30(8)-133.62(8)^o, defining a significantly distorted tetrahedron. The Zn-N distance (2.090(2) Å for Zn2-N1) and the Zn-O bond lengths (ranging from 1.925(2) to

2.112(2) Å) are comparable to those found in compound **1**. A noteworthy aspect of **3** is the distance (3.047 Å) between two metal centers which is the shortest one in compounds **1**-**4**.

Compounds **1**-**3** exhibit infinite 2D 6^3 networks in which their hexagonal windows consist of the three-connected (Zn_2/Co_2) uninode and the ndc^{2-} tether. The removal of one alcohol arm on $teaH_3$ gives rise of the different coordination environments in binuclear units for **3**. It is also responsible for the inconsistent coordination modes of ndc^{2-} ligand. The observed coordination modes for ndc^{2-} ligand can be of three types (μ_4-$\kappa^1\kappa^1\kappa^1\kappa^1$, μ_2-$\kappa^1\kappa^1$ and μ_2-$\kappa^1\kappa^1\kappa^1\kappa^1$ in Chart 1). The former two are found in compound **3** and all modes in compound **1**-**2**. In despite of the chair-shaped configuration in **1**-**3**, the above-mentioned differences make the hexagonal windows deformable (Figure 3c). The deformations can be verified by the dimensional sizes of six edges. As measured between the midpoints of two metal centers, the approximate dimensions of the hexagonal windows are 12.89 (×2) Å×14.66 (×2) Å×15.25(×2) Å for **1**, 12.91 (×2) Å×14.76 (×2) Å×15.17(×2) Å for **2**, and 12.90 (×2) Å×12.95 (×2) Å×15.75(×2) Å for **3**. The voids in the hexagonal windows of **1**-**3** are occupied by lattice MeOH molecules and two binuclear units from two up-and-down layers (Figure S1a and S2a). No interpenetration is found in **1**-**2**. However, the absence for one alcohol arm of $deaH_2$ minimizes the bulk of Zn_2 unit so that compound **3** must extraordinarily resort to a three-fold interpenetrating network to meet the close packing requirements. Obviously, the layered structure in **3** is packed into supramolecular networks with an ABCABC sequence (Figure 3d and 4).

Crystal structure of compound 4. Changing $teaH_3$ to $deaH_2$ produced a unique 6^3 network with three-fold interpenetration in **3**. The three-connected node is indispensable to construct the 6^3 network. Compounds **1**-**3** only possess the binuclear units as a uninode. Hence, the tripodal btb^{3-} ligand is introduced into our system to investigate a binodal 6^3 network. Compound **4** crystallizes in a monoclinic system with space group $P2_1/n$. One btb^{3-} anion, one $teaH_2^-$ anion, two Co^{II} ions as well as three EtOH molecules are presented in the asymmetric unit of **4** (Figure 5a). Compound **4** has the trigonal-bipyramidal environment in one Co center similar to those in **1**-**2**. But, the tetrahedral geometry for another Co center is in agreement with that of **3**. The Co-N distance (2.147(3) Å for Co2-N1) and the Co-O bond lengths (ranging from 1.930(3) to 2.034(3) Å) are comparable to those found in compound **2**. The btb^{3-} ligand has a μ_4-$\kappa^1\kappa^1\kappa^1\kappa^1$ connection mode toward four Co^{II} ions (chart 1). Two COO^- groups adopt the monodentate manner (μ_1-κ^1) to coordinate with two Co^{II} ions from two different Co_2 units. The third carboxyl group shows the bidentate manner (μ_2-$\kappa^1\kappa^1$) to bridge two Co^{2+} centers from one Co_2 unit. Therefore, one btb^{3-} ligand is connected to three Co_2 units while each dinuclear unit is linked with six Co_2 units through three btb^{3-} linkers. In compound **4**, the Co_2 unit behaves as a tripod while the central benzene ring of btb^{3-} ligand act as a planar three-connected nodes (Figure 5b). Three branched benzene fragments of btb^{3-} ligand serve as the tethers so that the total net can be described as a binodal 6^3 topology. It should be noticeable that the hexagonal windows consist of (—Co_2 unit—btb—)$_3$ entity with a ship-shaped configuration (Figure 5c). The approximate dimensions are 9.65(×2) Å×10.66(×2)

Å×10.67(×2) Å. The window sizes are significantly smaller than those of **1-3** so that no interpenetration appears in **4**. However, compound **4** possesses more voids than **1-3** do in that only one Co_2 unit from adjacent 6^3 layer is embedded into the hexagonal window (Figure S3a). As calculated by PLATON, the solvent-accessible volume in the unit cell for **4** accounts for approximate 32.1% of the total cell volume. In despite of the ABAB layered arrangement, the distinct structure of **4** uses its spacious voids to generate two types of 1D channels (I and II in Figure 5d) along *b* axe. The II channels are large enough to accommodate bulky EtOH molecules.

All the compounds **1-4** feature a 6^3 net constructed from the binuclear units (M_2L) (L=$teaH_2^-$/$deaH^-$). The connective behavior for binuclear units is similar to the patterns in our previous report,[2d] but different from those found in other related polymers for the binuclear building blocks $[Cu_2(\mu\text{-}L)_2(H_2O)_n]^{2+}$,[11h] (when L=N,N'-dimethylethanolamine n=2, and L=N-methyldiethanolamine or N-butyldiethanolamine, n=0). There is an inversion center in the $[Cu_2(\mu\text{-}L)_2(H_2O)_n]^{2+}$ blocks so that their binuclear units are generated from two metal centers and two polyalcohol amines. Each metal atom is chelated by one polyalcohol amine molecule and bridged to another metal center through two μ_2-O atoms of polyalcohol amines. This symmetry-related situation merely provides the carboxylate linker with two coordination positions. The final structure must result in a 1D chain. In comparison, only one center in **1-4** is chelated by one polyalcohol amine molecule. The second metal atom is held together through bridging COO^- groups and one μ_2-O atom of polyalcohol amine. This pattern may create an opportunity for three-connection.

Therefore, compounds **1**-**4** should resort to a suitable 2D network rather than 1D chain.

Supramolecular networks: The most striking features in these four compounds are the supramolecular assembly of the 2D subnets into the diversified 3D networks (Figure 2, 4, and 6). In compounds **1**-**4**, the 6^3 subnets are defined as building blocks for supramolecular assembly. A pair of strong symmetry-related H-bonds between binuclear units provides the 6^3 building blocks with intermolecular interactions. "Supramolecular synthons" are composed of the 6^3 subnets and the symmetry-related H-bonds. For **1** and **2**, each binuclear unit is double-connected to another unit through two symmetry-related H-bonds (Figure 2a). The 6^3 layers are stacked by means of an ABAB arrangement in which every discrete A layer is H-bonded to two above-and-below B layers (Figure S1b). The binuclear units become a four-connected uninodes with a square-pyramidal conformation, which results in a distorted 3D diamond framework without interpenetration (Figure 2a and 2b). From the structure of **3**, it can be seen that the 6^3 layers are arranged via an ABCABC mode with a three-fold interpenetration. The supramolecular interactions between binuclear units are involved in three sets of three-fold interpenetrations. Specifically speaking, every discrete A layer in one set is anchored to B and C nets from two adjoining sets by duplicate H-bonds between two Zn_2 units (Figure S2b). The binuclear units are expanded into a four-connected uninodes with a seesaw-shaped conformation (Figure 4a), which is different from that of **1**-**2**. The strong H-bonds can extend every set of 6^3 networks into a general 3D diamond topology with three-fold interpenetration (Figure

4b and 4c). Compound **4** has a binodal 6^3 net in which the 6^3 layers adopt an ABAB arrangement. In contrast to the H-bonds of **1**-**3**, the unit-unit interactions in **4** are happened among three binuclear units (Figure 6a). Each binuclear unit on one layer is H-bonded to two binuclear ones from two above-and-below B layers (Figure S3b). Therefore, the binuclear unit can utilize H-bonds to extend its nodal number from 3 to 5. It is very interesting that hydrogen bonds link the Co_2 units into a zigzag chain along *b* axe (Figure 6b). Finally, the overall topological structure of **4** becomes a complex binodal net with three-connected and five-connected nodes (Figure 6c). The short Schläfli symbol is $(6^3)\cdot(6^9\cdot8)$. It is quite significant that the supramolecular networks for our system can be constructed from the defined subnets (6^3 net) through symmetry-related H-bonds between the binuclear units. This strategy toward supramolecular topological aesthetics is in process.

XRPD, IR and Thermal Analysis: The main peaks in the simulated XRPD pattern are present in the experimental trace for **1**-**4** (Figure S4). The match between simulated and experimental XRPD patterns for **1**-**3** is well, indicating the phase purity of the three products. There are several peaks in the simulated pattern that are not present in the observed trace for **4**, which may be due to the part loss of its crystallinity. And so, the as-synthesized sample is still regarded as a pure phase.

The infrared spectra (IR) of **1**-**4** are depicted in ESI Figure S5, and the important adsorption peaks are listed in the Experimental Section. There are somewhat differences in two IRs for isomorphous **1** and **2**. However, the main adsorption peaks are similar to each other. For four as-synthesized products, the strong adsorption

peaks at 1610 cm^{-1} for **1**, 1590 cm^{-1} for **2**, 1570 cm^{-1} for **3** and 1610 cm^{-1} for **4** should be assigned to the asymmetric resonance of carboxylate stretching bands. Peaks ranging from 1390 cm^{-1} to 1410 cm^{-1} can be attributed to the symmetric stretching vibrations of the carboxylate groups. In addition, the weak absorptions (2860 cm^{-1} for **1**, 2850 cm^{-1} for **2** and **4**, 2870 cm^{-1} for **3**) correspond to the symmetric resonance for $-CH_2$ bands of $teaH_2^-$/$deaH^-$ anions.

Thermogravimetric analyses were performed using a Pyris Diamond thermal analyser. Approximate 10mg of products **1**-**4** were heated under a N_2 atmosphere in the temperature range RT-800ºC at a heating rate of 10ºC min^{-1}. As shown in Figure S6, the TGA curves of **1**-**3** display the weight loss of one methanol molecule (for **1**, Observed: 6.22%, Calcd: 5.06%; for **2**, Observed: 7.12%, Calcd: 5.17%; and for **3**, Observed: 6.98%, Calcd 5.44%) at 100-220^oC. However, compound **4** shows the first weight loss at 80^oC corresponding to one ethanol molecule (Observed: 6.12%, Calcd: 5.96%). The remaining alcohol molecules and tea ligand are lost in continuous steps in the range of 120-500 °C, and it is difficult to assign each weight loss separately. The TGA analysis of **1**-**4** indicates their host frameworks can be stable to 120 °C.

N_2 adsorption: It can be seen from single-crystal X-ray analysis that the offset arrangement of 6^3 layers in **1**-**4** gives rise of different packing effect. The hexagonal windows have a large cavity (>1nm), in which free solvent molecules and binuclear units are embedded. However, large 1D channel is formed when binodal 6^3 net in **4** is constructed. Therefore, standard N_2 adsorption isotherms for four compounds were measured for studying their distinguishable arrangement. Before recording the

measurements, the four samples were activated at 120 °C for 6 h to remove the occluded solvent molecules under high vacuum. As shown in Figure 7, the N_2 adsorption isotherm of **4** is type **I**, indicative of permanent microporosity.[18] An appreciable adsorbed amount of 45.04 $cm^3 g^{-1}$ at 0.40 P/P_0 and 77 K can be detected. A plateau of the large uptake can be retained near the saturation region. However, samples **1-3** do not show appreciable N_2 uptake, and the maximum adsorption at approximately 1 atm is 12.36 $cm^3 g^{-1}$. This difference in sorption properties is obviously generated from their different stacking behavior for 6^3 layers.

Conclusion

In summary, we succeeded in synthesizing four related coordination polymers with 6^3 net. The 6^3 subnet and the symmetry-related unit-unit H-bonds are regarded as supramolecular synthons to build up different supramolecular networks. We demonstrate the feasibility of crystal engineering on exploring supramolecular topology derived from the predefined subnets.

Acknowledgements

This work was supported by the NSF of China (grant No. 21201040 and 51463002) and the Development Program of Science and Technology of the Education Department of Jiangxi Province (grant No. GJJ14655).

Electronic supplementary information (ESI) available: XRD powder patterns, IR spectra, TGA curves. CCDC reference numbers 1045240-1045243. For ESI and crystallographic data in CIF or other electronic format see DOI:

References

1. (a) G. R. Desiraju, *Crystal Engineering: The Design of Organic Solids*; Elsevier: Amsterdam, The Netherlands, **1989**; (b) G. R. Desiraju, *J. Mole. Struct*. 2003, **656**, 5-15. (c) M. D. Allendorf, V. Stavila, *CrystEngComm*, 2015, **17**, 229-246.

2. (a) S. R. Batten, S. M. Neville and D. R. Turner, *Coordination Polymers: Design, Analysis and Application*, RSC Publishing, Cambridge, UK, **2009**; (b) L. J. Zhou, Y. Y. Wang, C. H. Zhou, C. J. Wang, Q. Z. Shi, S. M. Peng, *Cryst Growth Des*. 2007, **7**, 300-306; (c) E. Kim, H. Lee, T. H. Noh, O. S. Jung, *Cryst. Growth Des*. 2014, **14**, 1888-1894; (d) G. H. Xu, J. Y. Lv, P. Guo, Z. G. Zhou, Z. Y. Du, Y. R. Xie, *CrystEngComm*. 2013, **15**, 4473-4482.

3. (a) J. C. Mareque Rivas, L. Brammer, *Inorg. Chem*. 1998, **37**, 4756-4757. (b) A. Schoedel, M. Jaquier, W. Boyette, L. Wojtas, M. Eddaoudi, M. J. Zaworotko *Cryst Growth Des*, 2014, **14**, 2115-2117. (c) P. Bombicz, T. Gruber, C. Fischer, E. Weberb, A. Kálmána, *CrystEngComm*, 2014, **16**, 3646-3654.

4. G. R. Desiraju, *Angew. Chem., Int. Ed*. 2007, **46**, 8342-8356.

5. C. B. Aakeröy, N. R. Champness, C. Janiak, *CrystEngComm*. 2010, **12**, 22-43.

6. (a) K. Biradha, *CrystEngComm*. 2003, **5**, 374-384. (b) E. Bosch, Nathan. P. B, Jeffery. D, *Cryst. Growth Des*. 2015. **15**. DOI: 10.1021/cg5014076. (c) E. A. Mash, *CrystEngComm*, 2014, **16**, 8620-8637. (d) A. Mukherjee, S. Tothadi, G. R. Desiraju, *Acc. Chem. Res*, 2014, **47**, 2514-2524.

7. (a) L. Brammer, *Chem. Soc. Rev*. 2004, **33**, 476-489. (b) M. Mirzaei, H. Eshtiagh-Hosseini, Z. Karrabi, K. Molčanov, E. Eydizadeh, J. T. Mague, A. Bauzád, A. Frontera, *CrystEngComm*, 2014, **16**, 5352-5363. (c) G. Mukherjee, K.

Biradha *Cryst Growth Des*, 2014, **14**, 419-422.

8. J. Yang, J. F. Ma, S. R. Batten, *Chem. Commun*. 2012, **48**, 7899-7912.

9. Y. H. Deng, H. Liu, B. Yu, M. Yao, *Molecules*. 2010, **15**, 3478-3506.

10. (a) V. A. Blatov, *IUCr CompComm Newsletter*, 2006, 7, 4-38. http://www.topospro.com; (b) Three-letter symbols (lower case, bold) are used to characterize the nets in the RCSR (Reticular Chemistry Structure Resource). For example, **sql** for 4^4 net, **dia** for 6^6 net (namely the 3D diamond net). See: M. O'Keeffe, M. A. Peskov, S. J. Ramsden and O. M. Yaghi, *Acc. Chem. Res*. 2008, **41**, 1782-1789.

11. (a) G. H. Xu, X. Y. He, J. Y. Lv, Z. G. Zhou, Z. Y. Du, Y. R. Xie, *Cryst. Growth Des*. 2012, **12**, 3619-3630; (b) M. J. Manos, E. E. Moushi, G. S. Papaefstathiou, A. J. Tasiopoulos, *Cryst. Growth. Des*. 2012, **12**, 5471-5480; (c) W. G. Wang, A. J. Zhou, W. X. Zhang, M. L. Tong, X. M. Chen, M. Nakano, C. C. Beedle, D. N. Hendrickson, *J. Am. Chem. Soc*. 2007, **129**, 1014-1015; (d) T. Liu, Y. J. Zhang, Z. M. Wang, S. Gao, *J. Am. Chem. Soc*. 2008, **130**, 10500-10501; (e) D. Schray, G. Abbas, Y. H. Lan, V. Mereacre, A. Sundt, J. Dreiser, O. Waldmann, G. E. Kostakis, C. E. Anson, A. K. Powell, *Angew. Chem. Int. Ed*. 2010, **49**, 5185-5188; (f) S. M. Chen, J. Zhang, X. H. Bu, *Inorg. Chem*. 2009, **48**, 6356-6358. (g) A. M. Kirillov, Y. Y. Karabach, M. V. Kirillova, M. Haukka, A. J. L. Pombeiro, *Cryst. Growth Des*. 2012, **12**, 1069-1074; (h) S. S. P. Dias, V. André, J. Kłak, M. T. Duarte, A. M. Kirillov, *Cryst. Growth Des*. 2014, **14**, 3398-3407.

12. (a) T. Higashi, *ABSCOR*, Rigaku Corporation, Tokyo, Japan, **1995**; (b) G. M.

Sheldrick, *SADABS*, University of Göttingen, Germany, **1996**.

13. G. M. Sheldrick, *SHELXS-97*, *A Program for Automatic Solution of Crystal Structure*, University of Göttingen, Germany, **1997**.

14. G. M. Sheldrick, *SHELXL-97*, *A Program for Crystal Structure Refinement*, University of Göttingen, Germany, **1997**.

15. L. J. Farrugia, *WINGX, A Windows program for Crystal Structure Analysis*, University of Glasgow, UK, **1988**.

16. τ=(x-y)/60, where x is largest bond angle and y is second largest bond angle. For perfect trigonal bipyramid, τ is 1. See: A. W. Addison, T. N. Rao, *Dalton. Trans*. 1984. 1349-1356.

17. H. Z. Follner, *Anorg. Allg. Chem*. 1972, **387**, 43-51.

18. A. C. Sudik, A. R. Millward, N. W. Ockwig, A. P. Côté, J. Kim, O. M. Yaghi, *J. Am. Chem. Soc*. 2005, **127**, 7110-7118.

Table 1. Crystal data collections and structure refinements for compounds **1-4**.

Compound	**1**	**2**	**3**	**4**
Formula	$C_{25}H_{27}NO_{10}Zn_2$	$C_{25}H_{27}NO_{10}Co_2$	$C_{23}H_{23}NO_9Zn_2$	$C_{39}H_{47}NO_{12}Co_2$
Fw	632.3	619.4	588.2	839.7
Cryst size[mm]	0.25×0.10×0.10	0.24×0.20×0.16	0.20×0.15×0.10	0.30×0.24×0.18
Space group	*P-1*	*P-1*	*P-1*	$P2_1/n$
a(Å)	10.134(5)	10.182(1)	10.706(1)	16.635(5)
b(Å)	11.529(5)	11.550(1)	11.234(1)	9.405(5)
c(Å)	11.698(5)	11.676(1)	11.467(1)	25.855(5)
α (deg)	107.863(5)	108.454(1)	93.608(1)	90

β(deg)	95.831(5)	96.560(2)	111.597(1)	96.657(5)
γ (deg)	92.552(5)	92.829(2)	107.995(1)	90
V(Å^3)	1290.0(10)	1288.6(2)	1195.0(1)	4018.0(3)
Z	2	2	2	4
R_{int}	0.0318	0.0137	0.0159	0.0625
F(000)	647.9	635.9	599.9	1751.7
Reflcns collcd	5400/3872	5045/4224	4662/3942	7907/5234
GOF on F^2	1.0420	1.0360	1.0560	1.0300
$R_1[I > 2\sigma(I)]$	0.0675	0.0497	0.0377	0.0883
wR_2	0.1046	0.1105	0.0766	0.1492

Table 2. Selected Bond Lengths [Å] and Angles [deg] for Compounds **1-4**[a]

Compound1			
N1-Zn2	2.164(3)	O1-Zn2	1.954(2)
O2-Zn1	2.036(2)	O4-Zn1	1.999(3)
O5-Zn1	2.309(3)	O6-Zn1	2.112(3)
O7-Zn1	1.940(3)	O7-Zn2	1.941(3)
O8-Zn2	2.045(3)	O9-Zn2	2.080(3)
O7-Zn1-O4	139.09(13)	O7-Zn1-O2	97.62(11)
O4-Zn1-O2	95.25(12)	O7-Zn1-O6	109.64(11)
O4-Zn1-O6	107.63(12)	O2-Zn1-O6	95.16(11)
O7-Zn1-O5	93.70(10)	O4-Zn1-O5	91.42(11)
O2-Zn1-O5	153.85(11)	O6-Zn1-O5	58.76(9)
O7-Zn2-O1	105.77(11)	O7-Zn2-O8	120.39(12)
O1-Zn2-O8	97.82(12)	O7-Zn2-O9	127.62(12)
O1-Zn2-O9	90.83(11)	O8-Zn2-O9	105.34(13)
O7-Zn2-N1	84.27(11)	O1-Zn2-N1	168.94(11)
O8-Zn2-N1	80.53(12)	O9-Zn2-N1	79.16(11)
Compound2			
N1-Co2	2.155(3)	O1-Co2	2.032(2)
O2-Co2	2.035(2)	O3-Co2	1.945(2)
O3-Co1	1.964(2)	O4-Co2	1.981(2)
O5-Co1	2.029(2)	O7-Co1	2.058(2)
O8-Co1	2.287(2)	O9-Co1	2.102(2)
O3-Co1-O5	98.92(10)	O3-Co1-O7	147.95(11)

O5-Co1-O7	93.57(11)	O3-Co1-O9	105.52(10)
O5-Co1-O9	96.83(9)	O7-Co1-O9	102.11(10)
O3-Co1-O8	92.49(9)	O5-Co1-O8	155.70(9)
O7-Co1-O8	87.81(9)	O9-Co1-O8	59.29(8)
O3-Co2-O4	104.71(9)	O3-Co2-O1	118.70(11)
O4-Co2-O1	97.87(10)	O3-Co2-O2	127.50(11)
O4-Co2-O2	92.81(10)	O1-Co2-O2	106.86(11)
O3-Co2-N1	83.49(10)	O4-Co2-N1	171.34(10)
O1-Co2-N1	80.21(11)	O2-Co2-N1	79.78(10)
Compound3			
N1-Zn2	2.090(2)	O1-Zn2	1.994(2)
O2-Zn1	1.973(2)	O3-Zn2	1.987(2)
O4-Zn1	1.972(2)	O5-Zn1	1.925(2)
O7-Zn1	1.947(2)	O7-Zn2	2.054(2)
O8-Zn2	2.112(2)		
O5-Zn1-O7	133.62(8)	O5-Zn1-O4	108.26(8)
O7-Zn1-O4	107.80(7)	O5-Zn1-O2	99.72(8)
O7-Zn1-O2	98.30(8)	O4-Zn1-O2	104.75(8)
O3-Zn2-O1	103.64(8)	O3-Zn2-O7	107.69(7)
O1-Zn2-O7	95.13(7)	O3-Zn2-N1	100.73(8)
O1-Zn2-N1	154.66(8)	O7-Zn2-N1	83.88(8)
O3-Zn2-O8	108.30(8)	O1-Zn2-O8	84.70(8)
O7-Zn2-O8	142.96(8)	N1-Zn2-O8	81.20(8)
Compound4			
N1-Co2	2.147(3)	O2-Co1#1	1.959(3)
O3-Co1	1.975(3)	O4-Co2	1.978(3)
O5-Co1#2	1.954(3)	O7-Co2	2.015(3)
O8-Co1	1.930(3)	O8-Co2	1.940(3)
O9-Co2	2.034(3)	Co1-O5#3	1.954(3)
Co1-O2#4	1.959(3)		
O8-Co1-O5#3	116.05(12)	O8-Co1-O2#4	111.83(11)
O5#3-Co1-O2#4	97.91(12)	O8-Co1-O3	108.75(11)
O5#3-Co1-O3	108.44(12)	O2#4-Co1-O3	113.65(12)
O8-Co2-O4	101.46(12)	O8-Co2-O7	127.20(15)
O4-Co2-O7	95.15(14)	O8-Co2-O9	114.37(13)
O4-Co2-O9	100.88(13)	O7-Co2-O9	110.93(16)
O8-Co2-N1	82.29(12)	O4-Co2-N1	174.98(13)
O7-Co2-N1	79.88(14)	O9-Co2-N1	80.38(14)

[a]Symmetry transformations used to generate equivalent atoms: For **4**: #1 x-1, y, z. #2

x-1/2, -y+1/2, z-1/2. #3 x+1/2, -y+1/2, z+1/2. #4 x+1, y, z.

Table 3. Strong hydrogen bonds for compounds **1-4** [Å and deg].[b]

D-H...A	d(D-H)	d(H...A)	d(D...A)	<(DHA)
Compound1				
O8-H01...O10	0.898(1)	1.639(1)	2.535(5)	177(4)
O9-H02...O6^{i}	0.893(1)	1.773(1)	2.660(4)	172(4)
O10-H03...O3	0.82	1.88	2.618(6)	148.8
Compound2				
O1-H01...O10	0.892(1)	1.666(1)	2.542(4)	167(4)
O10-H03...O6	0.82	1.93	2.680(5)	150.8
O2-H02...O9^{i}	0.893(1)	1.751(1)	2.643(3)	176(4)
Compound3				
N1-H1...O6^{i}	0.91	2.07	2.948(3)	160.7
O9-H02...O7^{ii}	0.82	1.98	2.781(3)	164.8
O8-H01...O9	0.857(2)	1.842(2)	2.682(3)	166(3)
Compound4				
O7-H01...O12	0.895(1)	1.708(1)	2.603(5)	178(5)
O10-H10A...O11	0.82	1.96	2.705(5)	149.9
O9-H02...O1^{i}	0.899(1)	1.702(1)	2.591(4)	170(4)
O11-H11...O6^{ii}	0.82	1.90	2.725(4)	178.7
O12-H12A...O10^{iii}	0.82	1.88	2.696(5)	175.3

[b]Symmetry transformations used to generate equivalent atoms: For **1**: i -x+1, -y+1, -z+1. For **2**: i -x+1, -y+1, -z+2. For **3**: i -x+1, -y, -z+1; ii -x, -y, -z. For **4**: i -x+1/2, y+1/2, -z+1/2; ii x+1/2, -y+1/2, z+1/2; iii -x+1, -y+2, -z+1.

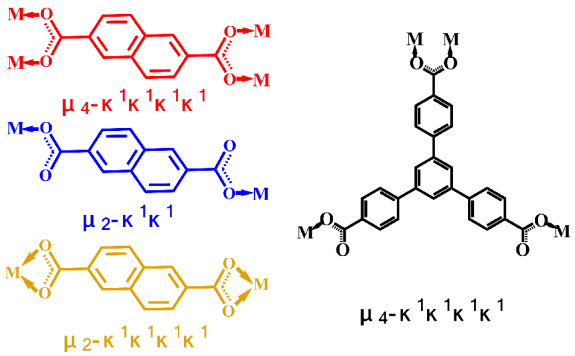

Chart 1. Observed coordination modes for organic carboxylate ligands. Three colors are used to identify the different coordination modes for ndc^{2-} anion (the same situation in Figure 1b, 1c, 3b and 3c).

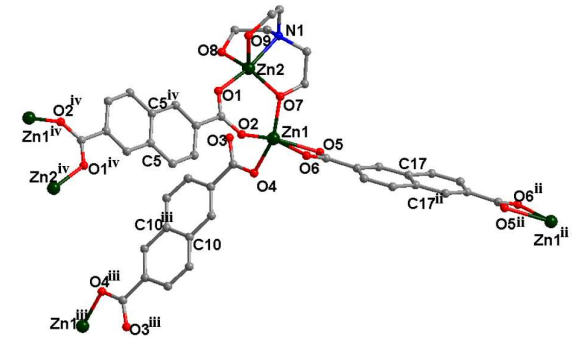

a

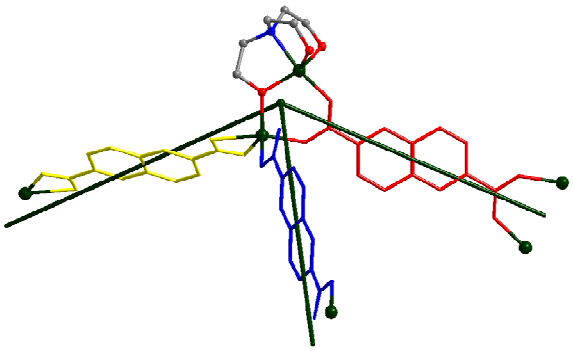

b

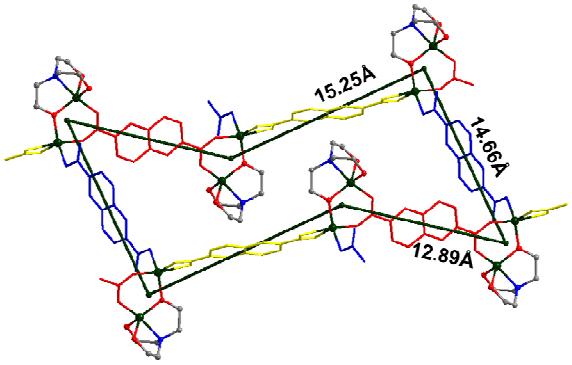

c

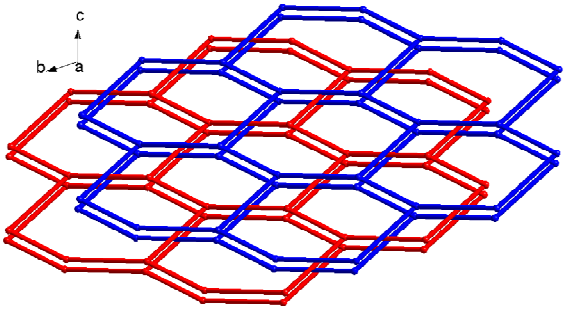

d

Figure 1. Crystal structure of **1**: a) the coordination environments of the Zn^{II} ions [Symmetry codes: ii -x+2, -y+2, -z+1; iii -x+2, -y, -z; iv –x+1, -y, -z+1]; b) a diagram of the Zn_2 unit behaving as a tripod with a schematic representation of the connectivity from the midpoint of two Zn^{II} ions; c) view of hexagonal window showing a chair-shaped configuration with detailed cavity sizes; d) the schematic view of an offset ABAB stacking arrangement for 6^3 layers.

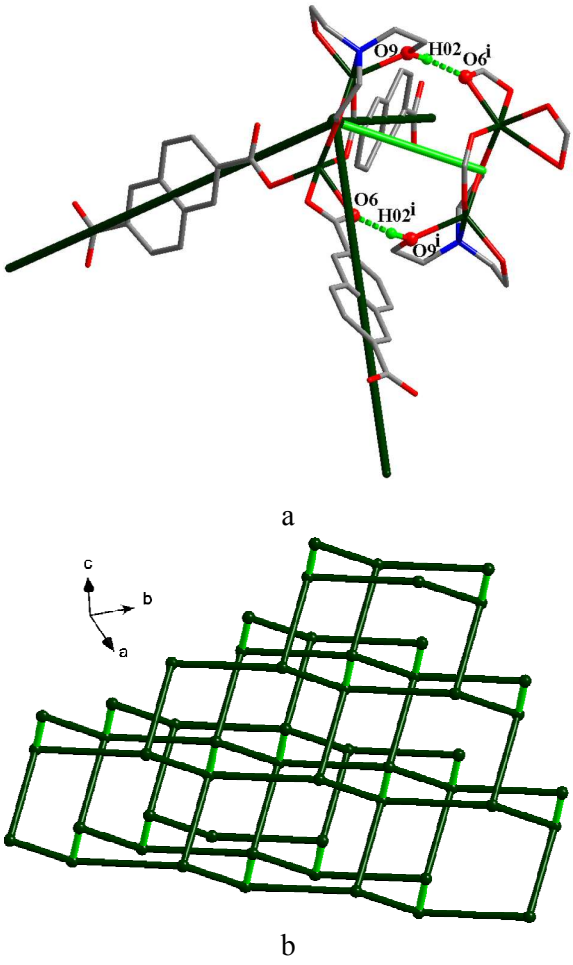

Figure 2. Supramolecular network of **1**: a) the symmetry-related H-bonds with atom-numbering details (dashed bright-green lines. Uninvolved H atoms have been omitted for clarity). The schematic connectivities from the midpoint of two Zn^{II} ions show a square-pyramidal conformation; b) the final supramolecular topology of

distorted diamond net constructed from the 6^3 subnet (dark-green lines) through H-bonds (bright-green lines).

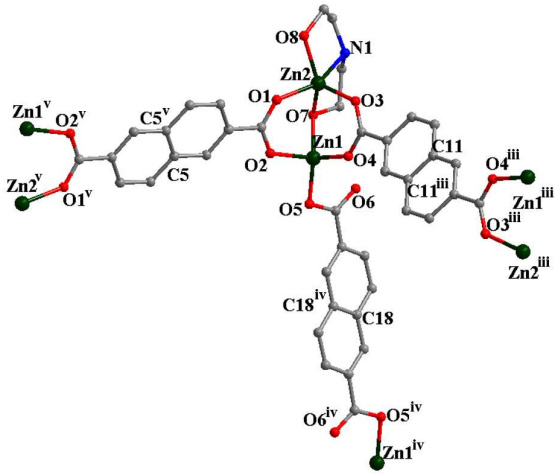

a

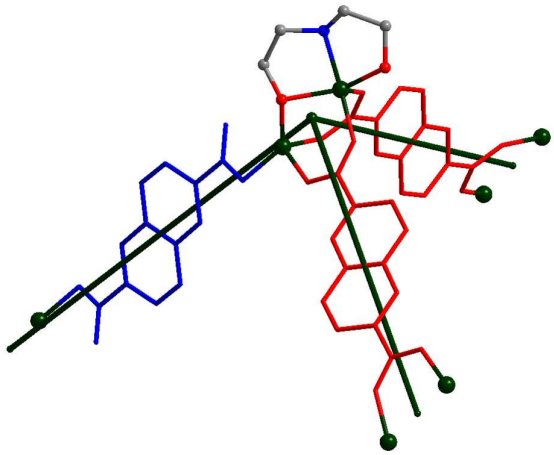

b

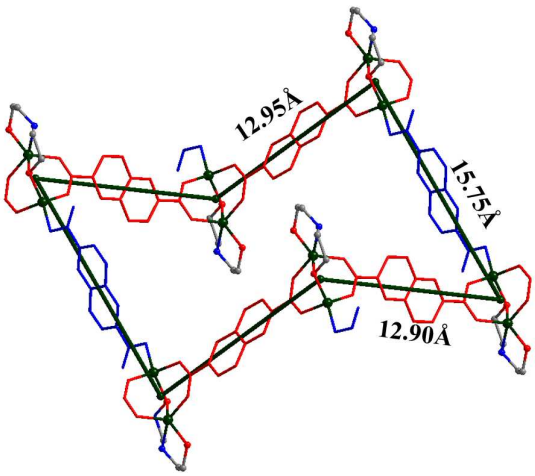

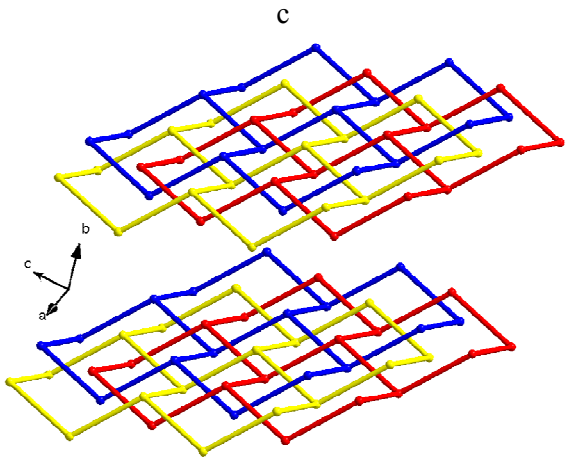

Figure 3. Crystal structure of **3**: a) the coordination environments of the Zn^{II} ions [Symmetry codes: iii -x+2, -y+1, -z+1; iv -x+1, -y+1, -z+2; v –x+1, -y+1, -z]; b) a diagram of the Zn_2 unit behaving as a tripod with a schematic representation of the connectivity from the midpoint of two Zn^{II} ions; c) view of hexagonal window showing a chair-shaped configuration with detailed cavity sizes; d) the schematic view of an offset ABCABC stacking arrangement for 6^3 layers due to the three-fold interpenetration.

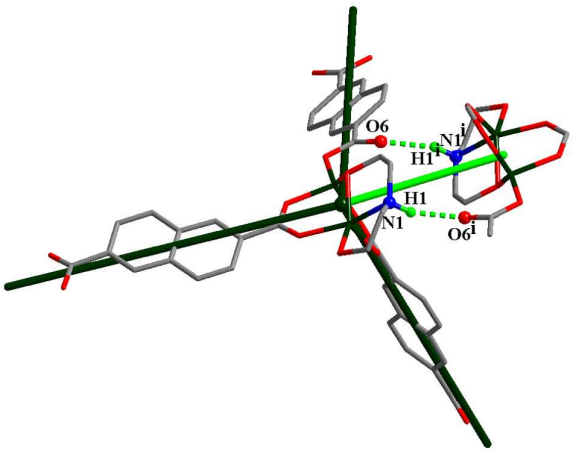

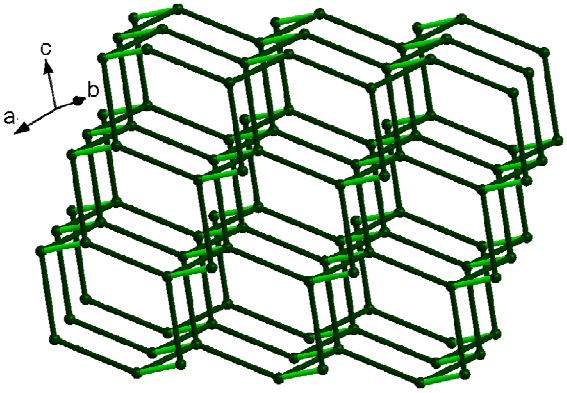

b

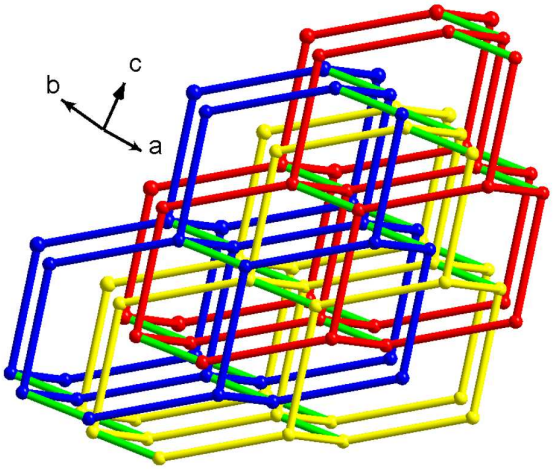

c

Figure 4. Supramolecular network of **3**: a) the symmetry-related H-bonds with atom-numbering details (dashed bright-green lines. Uninvolved H atoms have been omitted for clarity). The schematic connectivities from the midpoint of two Zn^{II} ions show a seesaw-shaped conformation; b) a general diamond net with the seesaw-shaped uninodes (bright-green lines for H-bonds); c) the final supramolecular topology of three-fold interpenetrating diamond net constructed from the 6^3 subnet (red, yellow, and blue lines) through H-bonds (bright-green lines).

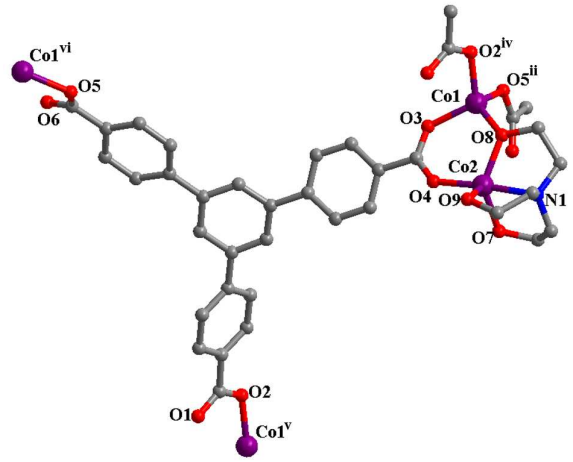

a

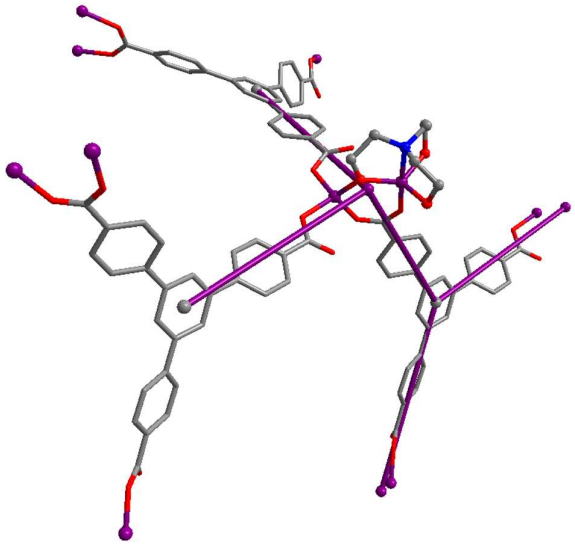

b

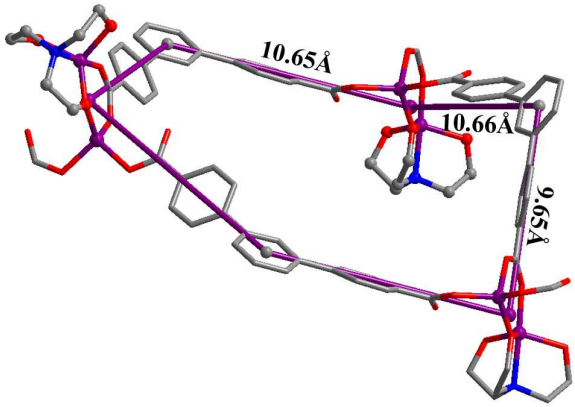

c

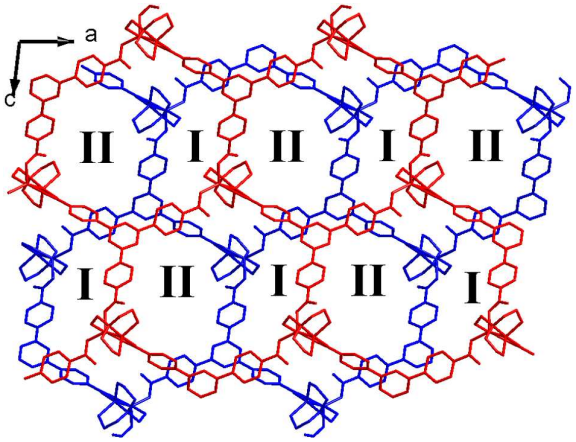

d

Figure 5. Crystal structure of **4**: a) the coordination environments of the Co^{II} ions [Symmetry codes: ii x+1/2, -y+1/2, z+1/2; iv x+1, y, z; v –x+1, y, z; vi x-1/2, -y+1/2, z-1/2]; b) a diagram of the binodes with a schematic representation of the connectivity between the midpoint of two Co^{II} ions and the centroid of central benzene ring of btb^{3-} ligand. The Co_2 unit behaving as a tripod while the central benzene ring of btb^{3-} ligand as a planar three-connected node; c) view of hexagonal window showing a ship-shaped configuration with detailed cavity sizes; d) the schematic view of an offset ABAB stacking arrangement for 6^3 layers, forming two types of 1D channels (the small **I** and the large **II**).

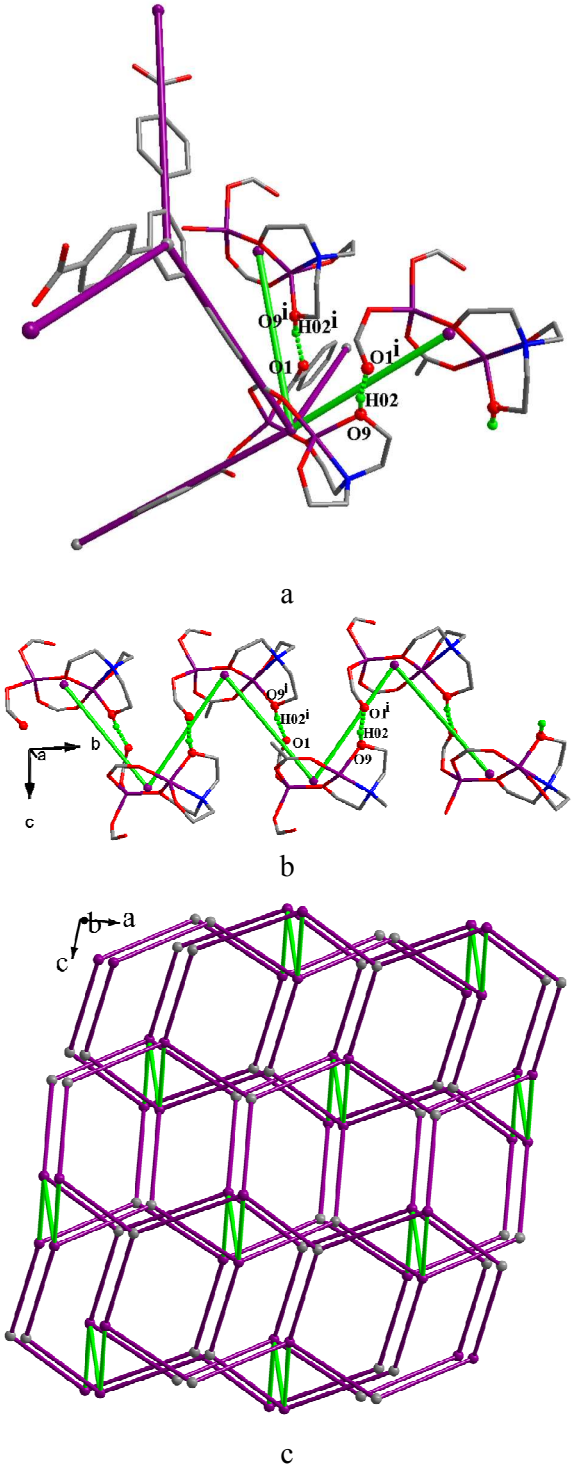

Figure 6. Supramolecular network of **4**: a) the symmetry-related H-bonds with atom-numbering details (dashed bright-green lines. Uninvolved H atoms have been omitted for clarity). The schematic representation shows a five-connected node for the

midpoint of two Co^{II} ions and a three-connected node for the centroid of central benzene ring of btb^{3-} ligand; b) 1D zigzag chain formed by H-bonding interactions between Co_2 units (bright-green lines for H-bonds); c) the final supramolecular topology of binodal $(6^3)\cdot(6^9\cdot8)$ net constructed from the 6^3 subnet (violet lines) through H-bonds (bright-green lines).

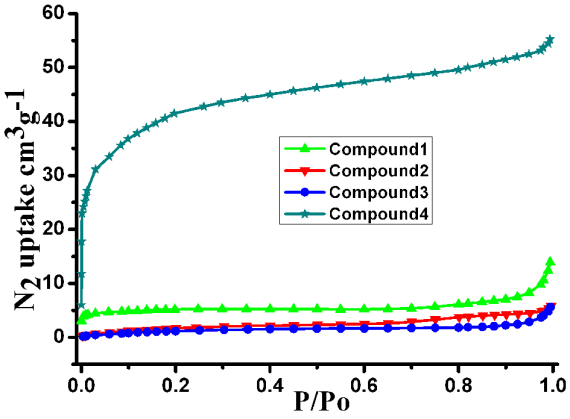

Figure7. N_2 sorption isotherms of samples **1**-**4** at 77 K

A Table of Contents Entry

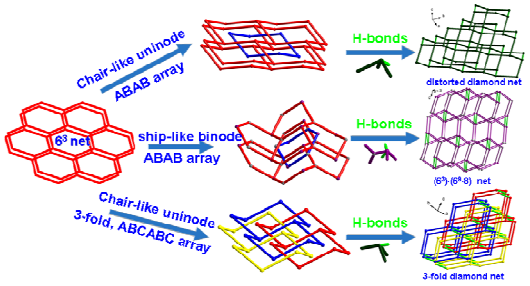

Text: This work reported four coordination polymers with 6^3 subnet and unit-unit H-bonds as supramolecular synthons to form different supramolecular networks.